Relaxation properties of (1 + 1)-dimensional driven interfaces in disordered media

2004 J. Phys. A: Math. Gen. 37 9621

(http://iopscience.iop.org/0305-4470/37/41/002)

J. Phys. A: Math. Gen. **37** (2004) 9621–9630 PII: S0305-4470(04)71839-9

Relaxation properties of (1 + 1)-dimensional driven interfaces in disordered media

A Díaz-Sánchez and A Pérez-Garrido

Departamento de Física Aplicada, Universidad Politécnica de Cartagena, Campus Muralla del Mar, Cartagena, E-30202 Murcia, Spain

E-mail: andiaz@upct.es

Received 13 November 2003
Published 29 September 2004
Online at stacks.iop.org/JPhysA/37/9621
doi:10.1088/0305-4470/37/41/002

Abstract

We use the Kardar–Parisi–Zhang equation with quenched noise in order to study the relaxation properties of driven interfaces in disordered media. For $\lambda \neq 0$ this equation belongs to the directed percolation depinning universality class and for $\lambda = 0$ it belongs to the quenched Edwards–Wilkinson universality class. We study the Fourier transform of the two-time autocorrelation function of the interface height $C_k(t', t)$. These functions depend on the difference of times $t - t'$ in the steady-state regime. We find a two-step relaxation decay in this regime for both universality classes. The long time tail can be fitted by a stretched exponential function, where the exponent β depends on the universality class. The relaxation time and the wavelength of the Fourier transform, where the two-step relaxation is lost, are related to the length of the pinned regions. The stretched exponential relaxation is caused by the existence of pinned regions which is a direct consequence of the quenched noise.

PACS numbers: 05.70.Ln, 68.35.Fx, 64.60.Ht

1. Introduction

Growing surfaces and interfaces moving in inhomogeneous media belong to the nonequilibrium statistical mechanics problems, which have attached much attention due to its importance in many fields, such as motion of liquids in porous media, growth of bacterial colonies, crystal growth, the motion of flux lines in superconductors or flame fronts [1]. Several models have been introduced in order to explain some experimental results [2–7]. In these models, inhomogeneous media are simulated by a quenched disorder which brakes the advancement of the interface. The continual motion of the interface requires the application of a driving force F. An analogy is possible with the theory of critical phenomena: there is a critical driving force F_c such that for driving forces below the critical one $F < F_c$ the advancement of the interface is halted after some finite time. This regime is called the pinning phase. While for $F > F_c$ the interface moves without stopping with an averaged velocity $v(F)$, this regime is the moving phase. As happens in critical phenomena, there is a phase transition at F_c, called the depinning transition, and the velocity plays the role of the order parameter. The characteristic length ξ of the pinned regions diverges at the transition and extends over the whole system in the pinning phase. A scaling behaviour is observed near to F_c and the values of the critical exponents lead to the classification of the models in universality classes.

A phenomenological nonlinear Langevin equation, the Kardar–Parisi–Zhang equation with quenched noise (QKPZ) [2] and the directed percolation depinning (DPD) models [3, 4] are the main models used to simulate driven interfaces in disordered media, which belong to the DPD universality class. The DPD models were proposed simultaneously by Tang and Leschhorn (TL model) [3] and Buldyrev *et al* [4]. The Kardar–Parisi–Zhang (KPZ) equation is

$$\partial_t h = F + \nu \nabla^2 h + \tfrac{1}{2}\lambda (\nabla h)^2 + \eta, \tag{1}$$

where the d-dimensional interface is described by a single-valued function $h(\mathbf{x}, t)$ which evolves in a $(d + 1)$-dimensional medium, ν and λ are constants, η is the noise and F is the driving force. When the noise depends on time (annealed noise) and $F = 0$, we have the KPZ equation [8]. If the noise does not depend on time (quenched noise) and $F \neq 0$, we have the QKPZ equation [2]. When $\lambda = 0$ in equation (1) and the noise is quenched this equation belongs to the Edwards–Wilkinson (QEW) universality class [5, 6]. Several models have been proposed to simulate driven interfaces belonging to QEW universality class [6, 7].

The relaxation process found in many glassy systems above the critical temperature has a two-step decay [9]. The long relaxation step has the stretched exponential form $f(t) = f_0 \exp[-(t/\tau)^{\beta}]$, where $0 < \beta < 1$ does not depend on the temperature. Two mechanisms driving nonexponential relaxation have been proposed in glassy systems [10, 11]. Both relate that behaviour to clusters of interactions. In the first mechanism, the clusters of interactions are a direct consequence of the quenched disorder [12], while in the other one, disorder is not needed to obtain nonexponential relaxation [13]. Colaiori and Moore [14] have found a stretched exponential relaxation for the KPZ equation in the mode-coupling approximation and given scaling functions [15]. In the TL model, the stretched exponential relaxation is found in the steady-state regime where the clusters of pinned cells (pinned regions) are responsible for this behaviour [16].

In this paper, we investigate the relaxation of the two-time autocorrelation function in the steady-state regime for the DPD and QEW universality classes. For that we perform numerical integration of equation (1) with quenched noise in 1 + 1 dimensions with $\lambda \neq 0$ for the DPD universality class and $\lambda = 0$ for the QEW universality class. We relate the relaxation properties to the pinned regions. The paper is organized as follows. In section 2 we review some properties of the pinned regions. In section 3 we present the model and the autocorrelation functions. The steady-state relaxation is studied in section 4 for both universality classes. Finally, in section 5, we present some conclusions.

2. Pinned regions

In the moving phase, when $F \to F_c^+$ a typical pinned region extends over a length of the order of $\xi_\parallel$ in the direction parallel to the interface and a length of the order of $\xi_\perp$ in the direction perpendicular to the interface. On both sides of the depinning transition, the two lengths have a power-law behaviour

$$\xi_\parallel \sim |g|^{-\nu_\parallel}, \qquad \xi_\perp \sim |g|^{-\nu_\perp},$$

where $\nu_{\parallel}$ is the parallel correlation length exponent, $\nu_{\perp}$ the perpendicular correlation length exponent and $g \equiv (F - F_c)/F_c$ the reduced driving force. The two lengths are connected by $\xi_{\perp} \sim \xi_{\parallel}^{\nu_{\perp}/\nu_{\parallel}}$. There is a saturation time, $t_s(L)$, which depends on the system size L, $t_s \sim L^z$, where z is the dynamical exponent. For $t \gg t_s$ the roughness reaches its saturation value, $W_{\text{sat}} \sim L^{\alpha}$, where α is the roughness exponent [6]. When $t \gg t_s$, the mean interface height has a linear behaviour $H = vt$ and the steady-state velocity vanishes for $F \to F_c^+$ as

$$v \sim g^{\theta}, \tag{2}$$

where θ is the velocity exponent [6]. Since, close to the transition $\xi_{\parallel} \sim L$, we have

$$v \sim h/t \sim \xi_{\perp}/t_s \sim \xi_{\perp}/L^z \sim \xi_{\perp}/\xi_{\parallel}^z \sim g^{z\nu_{\parallel}-\nu_{\perp}}, \tag{3}$$

leading to

$$\theta = z\nu_{\parallel} - \nu_{\perp}. \tag{4}$$

From $\theta = \nu_{\parallel}(z - \alpha)$ obtained in [6] and equation (4) we arrive at $\alpha = \nu_{\perp}/\nu_{\parallel}$.

For the DPD universality class in $1+1$ dimensions we have the following critical exponents [3, 6]: $\nu_{\parallel} = 1.73 \pm 0.04$, $\nu_{\perp} = 1.09 \pm 0.01$ and $z \approx 1$. Then, equation (4) takes the form given in [3]: $\theta = \nu_{\parallel} - \nu_{\perp}$. For the QEW universality class we have the following critical exponents [6]: $\nu_{\parallel} = 1.35 \pm 0.04$, $\nu_{\perp} = 1.66 \pm 0.04$ and $z = 1.45 \pm 0.07$.

3. Model and autocorrelation functions

Equation (1), in $1+1$ dimensions, takes the following form:

$$\partial_t h = F + \nu\partial_x^2 h + \tfrac{1}{2}\lambda(\partial_x h)^2 + \eta(x, h), \tag{5}$$

where the surface height $h = h(x, t)$ depends on the one-dimensional coordinate x and the time, F is the driving force, ν and λ are constants and the quenched noise η depends on the one-dimensional coordinate x and the height h. The details of the numerical integration are given in the appendix.

We define the probability distribution function of the height difference across the interface as

$$C(z; t', t) = \frac{1}{L}\sum_j \delta[h_j(t') - h_j(t) - z]; \tag{6}$$

this quantity was previously studied in a somewhat different context by Leschhorn and Tang [17]. The Fourier transform of $C(z; t', t)$ in z is

$$C_k(t', t) = \frac{1}{L}\sum_j \mathrm{e}^{-\mathrm{i}[h_j(t') - h_j(t)]k}, \tag{7}$$

where k is the wave number. A numerical integration of equation (5) is performed and $C_k(t', t)$ is evaluated. We average $C_k(t', t)$ over 100 different realizations of the quenched noise η.

4. Steady-state relaxation

For long enough times, $t' \gg t_s$, equations (6) and (7) depend only on the difference of times $t - t'$; this is the steady-state regime where the mean interface height has a linear behaviour $H(t) = vt$. This regime is reached at longer times when we approach the critical driving force F_c.

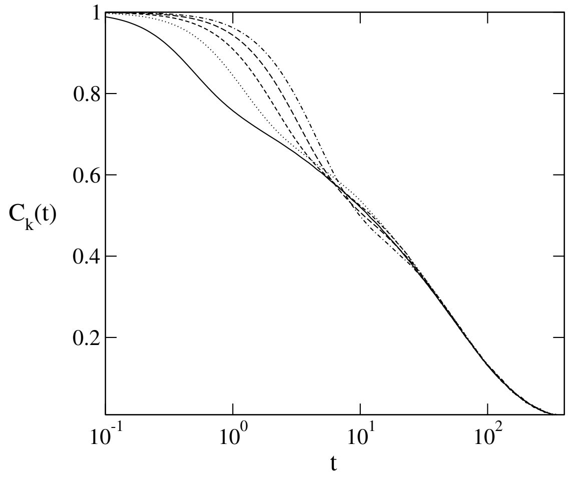

Figure 1. $C_k(t)$ in the steady-state regime for $\lambda = 1$, $F = 0.42$ and $k = \pi$ (solid line), $\pi/3$ (dotted line), $\pi/5$ (dashed line), $\pi/7$ (long dashed line) and $\pi/9$ (dot-dashed line).

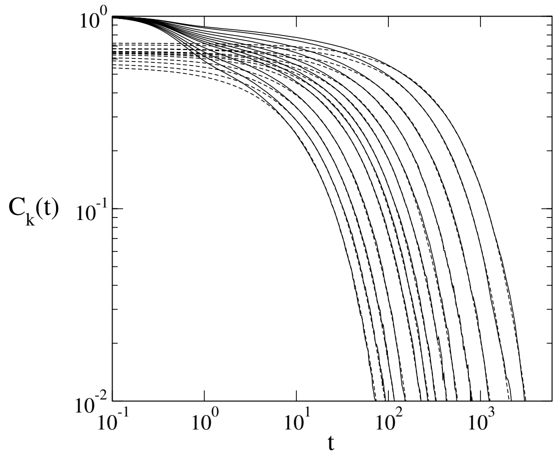

Figure 2. Log–log plot of $C_k(t)$ for $\lambda = 1$ where $k = \pi$ and $F = 0.52, 0.50, 0.48, 0.46, 0.44, 0.43, 0.42, 0.41, 0.40, 0.39, 0.38, 0.37$ and 0.365 (from left to right). Dashed curves are fitting functions corresponding to the stretched exponential functions.

4.1. DPD universality class

Equation (5) belongs to the $(1 + 1)$-dimensional DPD universality class when the constant $\lambda \neq 0$. In this case, we find a two-step relaxation decay in the steady-state regime. We can see in figure 1 that the time interval of the first and second relaxation steps depends on the wave number k. Nevertheless, the form of the second relaxation step does not depend on k. For small enough k we only have one-step relaxation process. So, there is a wave number k_e where the two-step relaxation decay is lost for $k < k_e$ and we can obtain a wavelength $\lambda_e = 2\pi/k_e$ in the direction perpendicular to the interface.

The time interval of the second step increases when F is decreased, i.e. when the system approaches criticality. As seen in figure 2, the second relaxation step can be fitted by a stretched

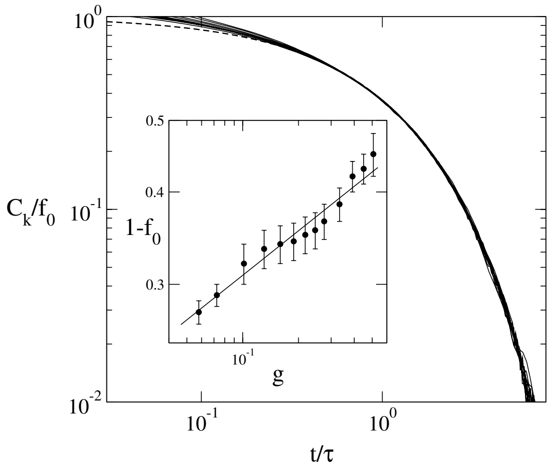

Figure 3. Scaling plot of $C_k(t)$; the dashed curve is a stretched exponential function with $\beta = 0.8$. Inset: log–log plot of the prefactor $1 - f_0$ as a function of g. The solid curve is a power-law function $1 - f_0 = 0.49g^{0.2}$.

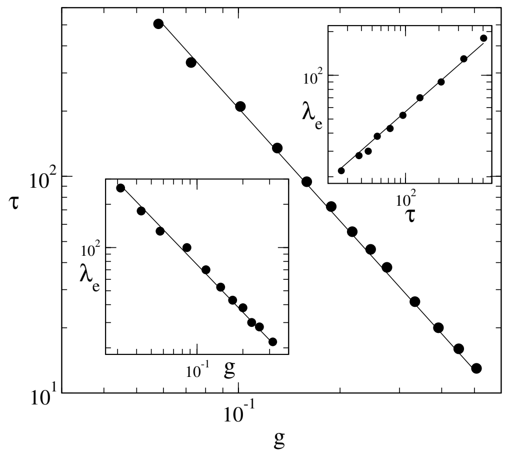

Figure 4. Log–log plot of the relaxation time τ, obtained by the stretched exponential fit in figure 3, as a function of g. The solid curve is a power-law function $\tau = 3.8g^{-1.73}$. Left inset: log–log plot of λ_e as a function of g for $F = 0.46$, 0.44, 0.43, 0.42, 0.41, 0.40, 0.39, 0.38, 0.37, 0.365 and 0.361. The solid curve is a power-law function $\lambda_e = 6.1g^{-1.1}$. Right inset: log–log plot of λ_e as a function of τ for $F = 0.46$, 0.44, 0.43, 0.42, 0.41, 0.40, 0.39, 0.38, 0.37 and 0.365. The solid curve is a power-law function $\lambda_e = 2.65\tau^{0.66}$.

exponential relaxation function, $f(t) = f_0 \exp[-(t/\tau)^{\beta}]$, with the exponent $\beta = 0.80 \pm 0.01$. This exponent is independent of F. The relaxation time τ and the prefactor f_0 are obtained from the scaling plot of $C_k(t)$ in figure 3. From the inset of figure 3 we propose the following scaling law for the prefactor f_0:

$$f_0 = 1 - A_0 g^{\kappa}, \tag{8}$$

with $A_0 = 0.49 \pm 0.05$, $\kappa = 0.20 \pm 0.05$ and $F_c = 0.345 \pm 0.005$.

In figure 4, we see that the relaxation time τ is very well fitted by a power law $\tau \sim g^{-\nu_{\parallel}}$ with $F_c = 0.345 \pm 0.005$ and $\nu_{\parallel} = 1.73 \pm 0.02$. This means that τ is proportional to the

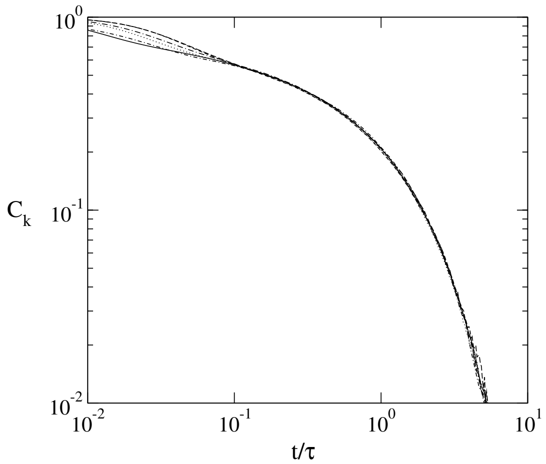

Figure 5. Log–log plot of $C_k(t)$ for $k = \pi$, with the same f_0 and different values for the constants of equation (5): $\lambda = 1$ and $\nu = 1$ (solid line), $\lambda = 1.5$ and $\nu = 1$ (dotted line), $\lambda = 2$ and $\nu = 1$ (dashed line), $\lambda = 2.5$ and $\nu = 1$ (long dashed line), $\lambda = 5$ and $\nu = 2$ (dot-long dashed line) and TL model obtained in [16] (dot-dashed line).

characteristic length of the pinned regions in the direction parallel to the interface, $\xi_\parallel$, which also diverges with the same exponent.

In figure 4 (left inset), we show λ_e as a function of g. This length diverges as a power law $\lambda_e \sim g^{-\nu_\perp}$ with $F_c = 0.350 \pm 0.005$ and $\nu_\perp = 1.10 \pm 0.03$, so that λ_e is proportional to the characteristic length of the pinned regions in the direction perpendicular to the interface, $\xi_\perp$, which also diverges with the same exponent. From $\tau \sim \xi_\parallel$, $\lambda_e \sim \xi_\perp$ and $\xi_\perp \sim \xi_\parallel^\alpha$, we have $\lambda_e \sim \tau^\alpha$; in figure 4 (right inset), we can see λ_e as a function of τ, with $\alpha = 0.66 \pm 0.01$.

We see that the characteristic length of the pinned regions in the direction parallel to the interface, $\xi_\parallel$, sets the time scale of the stretched relaxation function. On the other hand, the stretched relaxation step is lost for wavelengths larger than λ_e, i.e., for wavelengths $\lambda \gtrsim \xi_\perp$. So, the stretched exponential relaxation is caused by the pinned regions. From the fit of our results we have the following scaling function for the second relaxation step of $C_k(t)$:

$$C_k(t) = (1 - A_0 g^\kappa) \exp[-(A_1 g^{\nu_\parallel} t)^\beta], \tag{9}$$

where $A_0 = 0.49 \mp 0.02$ and $A_1 = 0.26 \mp 0.01$ are constants obtained from the fit in figure 3. From the results obtained for the TL model in [16], we have the same scaling function for this model but with $\kappa = 0.25 \pm 0.03$, $\nu_\parallel = 1.733 \pm 0.001$, $\beta = 0.805 \pm 0.005$, $A_0 = 0.65 \mp 0.05$ and $A_1 = 0.95 \mp 0.03$. The TL model and the QKPZ equation belong to the DPD universality class and the exponents obtained in equation (9) are the same within the errors for both models. In order to check if the β exponent depends on the details of the model or it is universal, we plot in figure 5 $C_k(t)$ for different values of the constants $\lambda \neq 0$ and ν in equation (5) and also for the TL model obtained in [16]. We choose all of them with the same prefactor f_0. It is shown that the second relaxation step is fitted very well with the stretched exponential function with $\beta = 0.80 \pm 0.01$.

4.2. *QEW universality class*

Equation (5) belongs to the (1 + 1)-dimensional QEW universality class when the constant $\lambda = 0$. The results obtained in this case are similar to the ones found for the DPD universality

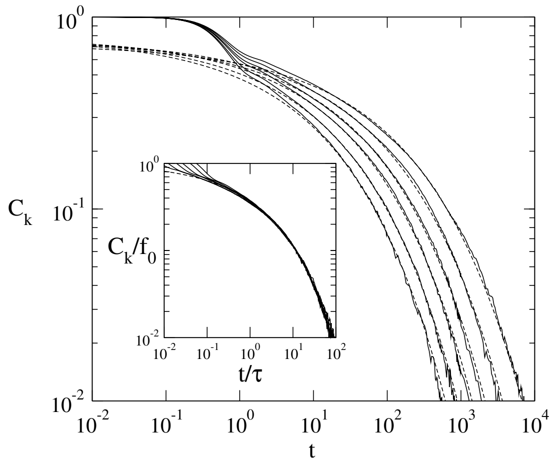

Figure 6. Log–log plot of $C_k(t)$ for $\lambda = 0$ where $k = \pi$ and $F = 1.01$, 1.006, 1.003, 1.00, 0.998 and 0.996 (from left to right). Dashed curves are fitting functions corresponding to the stretched exponential functions. Inset: scaling plot of $C_k(t)$ with $f_0 = 0.76 \pm 0.01$. The dashed curve is a stretched exponential function with $\beta = 0.34$.

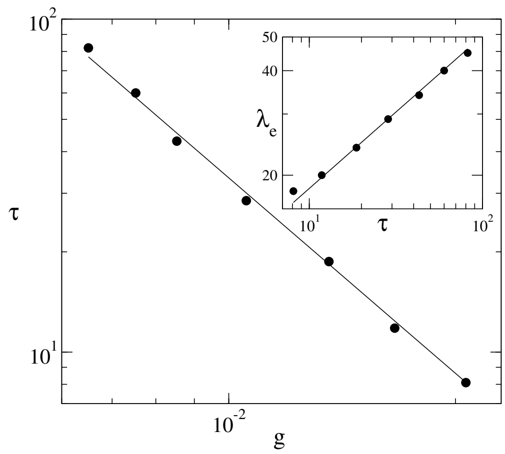

Figure 7. Log–log plot of the relaxation time τ, obtained by the stretched exponential fit in figure 6, as a function of g for $F = 1.01$, 1.006, 1.003, 1.00, 0.998, 0.997 and 0.996. The solid curve is a power law function $\tau = 0.0042g^{-1.95}$. Inset: log–log plot of λ_e as a function of τ, for $F = 1.01$, 1.006, 1.003, 1.00, 0.998, 0.997 and 0.996. The solid curve is a power law function $\lambda_e = 6.65\tau^{0.44}$.

class. We obtain a two-step relaxation decay where the second step can be fitted by the stretched exponential function, as seen in figure 6. The value of the exponent $\beta = 0.34 \pm 0.01$ does not depend on F and the prefactor $f_0 = 0.76 \pm 0.01$ is practically constant for the range of F studied here.

Figure 6 (inset) shows the scaling plot of C_k. From this scaling fit, we obtain the relaxation time τ which follows a power-law divergency $\tau \sim g^{-1.95\pm0.05}$ with $F_c = 0.990 \pm 0.008$ (figure 7). We expect that $\tau \sim t_s \sim \xi_\parallel^z$ with τ the time scale of the relaxation function, then $\tau \sim g^{-z\nu_\parallel}$ where $z\nu_\parallel \approx 1.95 \pm 0.15$ [6], as obtained in figure 7. Figure 7 (inset) shows λ_e as a function of τ which follows a power law $\lambda_e \sim \tau^\gamma$ with $\gamma = 0.44 \pm 0.01$.

We see that the time scale of the stretched relaxation function is set by a power of the characteristic length of the pinned regions in the direction parallel to the interface, $\xi_{\parallel}^{z}$. On the other hand, a simple relation between the other parameters of the relaxation and the static properties of the pinned regions does not exist.

The scaling function for the second relaxation step of $C_k(t)$ is

$$C_k(t) = f_0 \exp[-(A_1 g^{z\nu_{\parallel}} t)^{\beta}], \tag{10}$$

where $f_0 = 0.76 \mp 0.01$ and $A_1 = 238 \mp 1$ are constants obtained from the fit in the inset of figure 6. We also obtain the same value of the β exponent for the constant $\lambda = 0$ and different values of the constant ν in equation (5). So, the exponent β of the stretched relaxation step depends on the universality class.

5. Conclusions

We have studied relaxation properties for driven interfaces in disordered media in $1+1$ dimensions. We have used the QKPZ equation ($\lambda \neq 0$ in equation (5)) and the QEW equation ($\lambda = 0$ in equation (5)) and studied the relaxation properties of the Fourier transform of the autocorrelation of the surface height. A two-step relaxation process is found in both models. The second relaxation step is well fitted by a stretched exponential function with $\beta = 0.80 \pm 0.01$ in the DPD universality class and $\beta = 0.34 \pm 0.01$ in the QEW universality class. This exponent depends on the universality class of the model. The relaxation time diverges as a power law in both universality classes. In the DPD universality class, this relaxation time is proportional to the characteristic length of the pinned regions in the direction parallel to the interface, $\xi_{\parallel}$. On the other hand, in the QEW universality class, it is proportional to $\xi_{\parallel}^{z}$, so it grows faster than $\xi_{\parallel}$. The form of the second relaxation step does not depend on the wave number of the Fourier transform. In the DPD universality class, this step vanishes for a given wavelength λ_e, which is proportional to the characteristic length of the pinned regions in the direction perpendicular to the interface, $\xi_{\perp}$. On the other hand, in the QEW universality class, a simple relation between the others parameters of the relaxation and the static properties of the pinned regions does not exist. Thus, the stretched exponential relaxation behaviour is caused by the pinned regions, which appear as a direct consequence of the quenched noise.

Acknowledgments

We acknowledge SEDIC for the allocation of computer resources. This work was supported in part by the project no. PI-60/00858/FS/01 from the Fundación Séneca Región de Murcia.

Appendix

We perform the numerical integration of the equation (5) using finite-difference methods [18–20]:

$$h(x_j, t + \Delta t) = h(x_j, t) + \Delta t \left[\nu \partial_x^2 h + \frac{\lambda}{2} (\partial_x h)^2 \right]_{x_j} + \Delta t \; \eta(x_j, h). \tag{A.1}$$

In the operators containing spatial derivatives, we introduce their finite-difference approximations. For the operator $\partial_x^2 h$ we use the approximation with error $O((\Delta x/L)^4)$, instead the one used in [18–20], which has error $O((\Delta x/L)^2)$, where L is the lateral size of the system,

$$\partial_x^2 h = \frac{1}{12\Delta x^2}[-h(x_j - 2\Delta x, t) + 16h(x_j - \Delta x, t) - 30h(x_j, t) + 16h(x_j + \Delta x, t) - h(x_j + 2\Delta x, t)]. \tag{A.2}$$

For the nonlinear term, we use the finite-difference approximations with error $O((\Delta x/L)^4)$ for $\partial_x h$

$$(\partial_x h)^2 = \left(\frac{1}{12\Delta x}[-h(x_j - 2\Delta x, t) + 8h(x_j - \Delta x, t) - 8h(x_j + \Delta x, t) + h(x_j + 2\Delta x, t)]\right)^2. \tag{A.3}$$

With these approximations we have convergency of our integrations using a Δt larger than with the approximations of error $O((\Delta x/L)^2)$ used in [18–20]. As in [20] we take the linear interpolation of the noise term into account

$$(1 - p)\eta(x, [h(x, t)]) + p\eta(x, [h(x, t)] + 1), \tag{A.4}$$

where $[\ldots]$ denotes the integer part, with $p = h(x, t) - [h(x, t)]$.

We work with square lattice systems of edge $L = 10\,000$, $\Delta x = 1$ and periodic boundary conditions in the x-direction. η is uniformly distributed in $[-a/2, a/2]$ with $a = 10^{2/3}$; the conclusions of this paper are independent of a and the same results in the universal findings are obtained if a Gaussian distribution is chosen. We use $\Delta t = 0.01$ (with this choice we ensure the convergency of the results). The initial condition is $h(x, 0) = 0$. The averages are taken over 100 different realizations of quenched noise.

References

[1] Family F and Vicsek T (ed) 1991 *Dynamics of Fractal Surfaces* (Singapore: World Scientific)
Meakin P 1993 *Phys. Rep.* **235** 189
Kertész J and Vicsek T 1994 *Fractals in Science* ed A Bunde and S Havlin (Heidelberg: Springer)
Halpin-Healey T and Zhang Y C 1995 *Phys. Rep.* **254** 215
Barabási A L and Stanley H E 1995 *Fractal Concepts in Surface Growth* (Cambridge: Cambridge University Press)

[2] Tang L H, Kardar M and Dhar D 1995 *Phys. Rev. Lett.* **74** 920

[3] Tang L H and Leschhorn H 1992 *Phys. Rev.* A **45** R8309

[4] Buldyrev S V, Barabási A L, Caserta F, Havlin S, Stanley H E and Vicsek T 1992 *Phys. Rev.* A **45** R8313

[5] Grinstein G and Ma S K 1983 *Phys. Rev.* B **28** 2588
Nattermann T, Stepanov S, Tang L H and Leschhorn H 1992 *J. Phys. II (France)* **2** 1483
Narayan O and Fisher D S 1993 *Phys. Rev.* B **48** 7030

[6] Amaral L A N, Barabási A L and Stanley H E 1995 *Phys. Rev.* E **52** 4087

[7] Leschhorn H 1993 *Physica* A **195** 324

[8] Kardar M, Parisi G and Zhang Y C 1986 *Phys. Rev. Lett.* **56** 889

[9] Götze W 1991 *Liquids, Freezing and Glass Transition* ed J P Hansen, D Levesque and P Zinn-Justin (Amsterdam: Elsevier)

[10] Randeria M, Sethna J P and Palmer R G 1985 *Phys. Rev. Lett.* **54** 1321
Cesi F, Maes C and Martinelli F 1997 *Commun. Math. Phys.* **188** 135
Franzese G and Coniglio A 1998 *Phys. Rev.* E **58** 2753

[11] Fortuin C M and Kasteleyn P W 1972 *Physica (Amsterdam)* **57** 536
Coniglio A and Klein W 1980 *J. Phys. A: Math. Gen.* **12** 2775

[12] Fierro A, de Candia A and Coniglio A 1997 *Phys. Rev.* E **56** 4990

[13] Fierro A, Franzese G, de Candia A and Coniglio A 1999 *Phys. Rev.* E **59** 60

[14] Colaiori F and Moore M A 2001 *Phys. Rev.* E **63** 057103

[15] Colaiori F and Moore M A 2001 *Phys. Rev. Lett.* **86** 3946

[16] Díaz-Sánchez A, Pérez-Garrido A, Urbina A and Catalá J D 2002 *Phys. Rev.* E **66** 031403
[17] Leschhorn H and Tang L H 1994 *Phys. Rev.* E **49** 1238
[18] Csahók Z, Honda K, Somfai E, Vicsek M and Vicsek T 1993 *Physica* A **200** 136
[19] Jeong H, Kahng B and Kim D 1999 *Phys. Rev.* E **59** 1570
[20] Díaz-Sánchez A, Braunstein L A and Buceta R C 2001 *Eur. Phys. J.* B **21** 289